Enhanced Optical and Electrical Characteristics of Si Detectors Integrated with Periodic 1-D and 2-D Semiconductor Nanoscale Structures

A. K. Sharma[a], S. H. Zaidi[b], G. Liecthy[a], and S. R. J. Brueck[c]
[a]Air Force Research Laboratory/VSSE, 3550 Aberdeen Ave., SE, Kirtland AFB, NM 87117
ashwani.sharma@kirtland.af.mil
[b]Gratings Inc., Albuquerque, NM 87107
[c]Center for High Technology Materials, University of New Mexico, Albuquerque, NM 87106

Abstract

Nanostructuring the active region of metal-silicon-metal (MSM) photodetectors (PDs) with sub-wavelength periodic 1-D and 2-D nanoscale grating structures significantly modifies the optical absorption, reflectance and transmission properties of silicon. These modifications dramatically impact the electrical characteristics of the MSM PDs. The surface reflection is reduced from ~33% (planar Si) to ~4% (nanostructured Si) for triangular shaped nanostructures. The internal quantum efficiency of the MSM PDs increased from ~63% (planar) to ~80% (nanostructured) at λ=700nm. Also a faster time constant (~1700ps for planar MSM PD to ~600ps for nanostructured MSM PD was achieved by enhancing the optical absorption near the surface where the carriers are efficiently and rapidly collected.

1. Introduction

Si photodetectors operate over a wide spectral range across the UV, visible, and near IR regions, and are used for varied applications in radiometry, photometry, calorimetry, and imaging [1]. In recent years, Si photodetectors have been proposed as receivers in fiber optics communication applications. There is considerable interest in the near IR wavelength (λ=770-850 nm) applications due, in part, to the lower cost of diode laser systems. At these wavelengths, both Si and GaAs are viable candidates for fabrication of monolithically integrated optical receivers [2]. GaAs is attractive due to its short absorption length (~1.0 μm at λ=850 nm), which makes it possible to have large bandwidth combined with good responsivity [3]. Si offers the potential of lower cost and direct integration with VLSI technology. A significant disadvantage lies in silicon's long absorption lengths (~15 μm at λ=850 nm) resulting in difficult trade-offs between responsivity and bandwidth. Si optoelectronic circuits with good sensitivity but poor response times have been reported [4]. Si MSM PDs with lateral interdigitated electrodes combine high speed with VLSI process compatibility. These detectors operate at very high frequencies in UV [5] and visible spectral range [6]. The electric field in a lateral MSM PD configuration decreases rapidly as a function of distance from the surface. In the near IR spectral range, most of the electron-hole pairs are generated in an undepleted region. The response speed of these devices is limited by carrier diffusion. Several attempts have been reported aimed at improving high-speed response and enhancing the near IR absorption. Improved high-speed response has been demonstrated using vertical [7] and U-shaped [8] trench electrodes using reactive ion and wet chemical etching mechanisms. These devices exhibit improved performance in comparison with planar contacts, however they still suffer from long carrier diffusion tails corresponding to carriers generated in the bulk Si region. Liu *et al.*[9], reported improved speed response by fabrication of MSM PDs on Si-on-insulator (SOI) substrates. The key feature in speed enhancement is the buried oxide layer that limits the active Si thickness, and prevents diffusion of bulk-generated carriers. Only the electron-hole pairs generated in the top, active Si layer are subject to high electric fields and contribute to the photocurrent. By reducing the Si film thickness to ~100 nm, they demonstrated photodetector bandwidth of 140 GHz at 780 nm wavelength, however, at the cost of very low quantum efficiency (~1%). Lee *et al.*[10] have proposed MSM PD configuration on 5-μm thick Si membrane. Geometrical texturing schemes were used for enhanced light trapping. Trapping of light in a thin membrane results in minimal reduction in responsivity, while reducing carrier transit times.

Here, we report on nanoscale structuring of Si aimed at promoting near IR absorption close to the surface using sub-wavelength nanostructured gratings. These nanoscale structuring techniques are based on physical optics considerations. A commonly used electromagnetic modeling approach of the reflection, transmission and absorption for periodic grating structures is the rigorous coupled wave analysis (RCWA) [11] method. This method is used here to predict the photocurrent enhancement of the MSM PDs integrated with nanostructured gratings in the active region.

0-7803-7215-8/01/$10.00©2001 IEEE.

Report Documentation Page

Form Approved
OMB No. 0704-0188

1. REPORT DATE	2. REPORT TYPE	3. DATES COVERED
2001		**-**

4. TITLE AND SUBTITLE	5a. CONTRACT NUMBER
Enhanced Optical and Electrical Characteristics of Si Detectors Integrated with Periodic 1-D and 2-D Semiconductor Nanoscale Structures	5b. GRANT NUMBER
	5c. PROGRAM ELEMENT NUMBER
6. AUTHOR(S)	5d. PROJECT NUMBER
A Sharma; S Zaidi; G Liecthy; S Brueck	5e. TASK NUMBER
	5f. WORK UNIT NUMBER
7. PERFORMING ORGANIZATION NAME(S) AND ADDRESS(ES)	8. PERFORMING ORGANIZATION REPORT NUMBER
Gratings Inc,2700 Broadbent Pkwy NE,Albuquerque,NM,87107	
9. SPONSORING/MONITORING AGENCY NAME(S) AND ADDRESS(ES)	10. SPONSOR/MONITOR'S ACRONYM(S)
	11. SPONSOR/MONITOR'S REPORT NUMBER(S)

12. DISTRIBUTION/AVAILABILITY STATEMENT

Approved for public release; distribution unlimited

13. SUPPLEMENTARY NOTES

14. ABSTRACT

Nanostructuring the active region of metal-silicon-metal (MSM) photodetectors (PDs) with subwavelength periodic 1-D and 2-D nanoscale grating structures significantly modifies the optical absorption, reflectance and transmission properties of silicon. These modifications dramatically impact the electrical characteristics of the MSM PDs. The surface reflection is reduced from ~33% (planar Si) to ~4% (nanostructured Si) for triangular shaped nanostructures. The internal quantum efficiency of the MSM PDs increased from ~63% (planar) to ~80% (nanostructured) at lambda=700nm. Also, a faster time constant (~1700 ps for planar MSM PD to ~600 ps for nanostructured MSM PD) was achieved by enhancing the optical absorption near the surface where the carriers are efficiently and rapidly collected.

15. SUBJECT TERMS

16. SECURITY CLASSIFICATION OF:			17. LIMITATION OF ABSTRACT	18. NUMBER OF PAGES	19a. NAME OF RESPONSIBLE PERSON
a. REPORT	b. ABSTRACT	c. THIS PAGE			
unclassified	**unclassified**	**unclassified**		**7**	

2. Device Fabrication

Interferometric lithography (IL) provides an inexpensive method for the fabrication of nanoscale periodic structures over large areas and is ideally suited for large-scale manufacturing [12]. Interference effects between two coherent laser beams produce a simple periodic pattern with period, $d=\lambda/2 \sin\theta$, where λ is the wavelength of the exposing beam, and 2θ is the angle between the two intersecting beams [13]. Fig. 1 shows a typical IL experimental configuration in which an expended and collimated laser beam is incident on a Fresnel mirror (FM) arrangement mounted on a rotation stage for period variation [14]. A mix and match process was used to localize the IL pattern at the desired locations [15]. After developing the resist, reactive ion etching (RIE) or wet chemical etching using potassium hydroxide (KOH) can be employed to transfer the pattern into the wafer. The Si substrate material used in the fabrication of the MSM PDs in this investigation was lightly n-type doped; the phosphorous (P) concentration was ~8 x 10^{14} cm^{-3}. No epitaxial growth was used. Typical 1-D and 2-D Si nanostructure configurations are shown in Fig. 2.

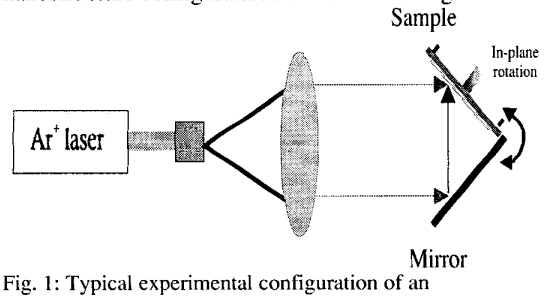

Fig. 1: Typical experimental configuration of an interferometric lithography setup.

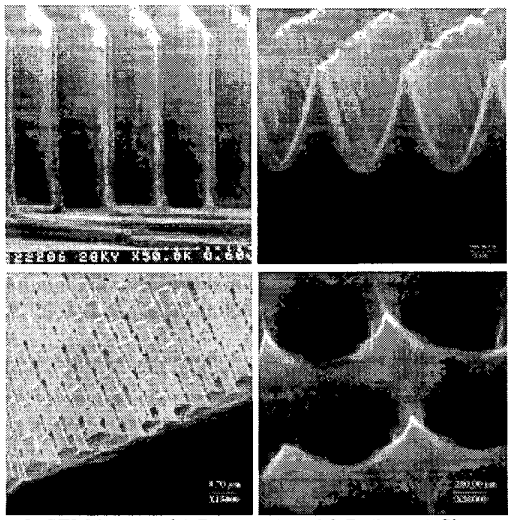

Fig. 2: SEM image of 1-D (upper) and 2-D (lower) Si nanostructure gratings.

Following Si etching, a rapid thermal anneal (RTA) process step was performed to anneal some of the damage created at the surfaces by the RIE [16]. Following the localized nanoscale texturing of the device active regions, the MSM PDs were fabricated using a 3-mask process. First, a low temperature evaporated SiO_2 isolation layer (~100-nm thick) was deposited. Windows defining the active regions were opened in the oxide using standard photolithography and buffered oxide etch (BOE). 50-nm thick Ni Schottky barrier electrodes were e-beam evaporated with gaps ranging from 5 to 20 μm and aspect ratios of 5:1 using lift-off. Thicker 50:300 nm Cr:Au bonding metallization was then evaporated for contact pads above the oxide using a third mask and again using lift-off. Ni Schottky barriers were used for convenience, but standard $W:Si_x$ Schottky barrier contacts could easily be substituted. This simple device geometry was chosen for ease of data analysis and device understanding. More complex, large area geometries can be generated for commercial applications. Fig. 3a & 3b show optical micrographs of complete structured MSM and planar MSM devices respectively. The active areas of the devices shown are 50 μm X 50 μm. The interdigitated electrode gaps are 10 μm. Note in Fig. 3a that the active area of the structured device is almost black due to very low surface reflection.

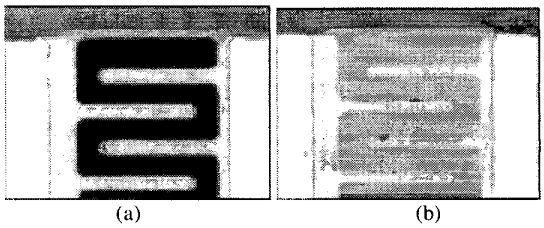

(a) (b)

Fig. 3: Optical micrographs of MSM Photodetector devices (a) nanostructured and (b) planar.

3. Modeling of Periodic Nanoscale Structures

Light interaction with nanoscale grating structures is a complex function of several parameters including the incident wavelength, angle, polarization, period, profile, and duty cycle [17]. For fast MSM PD applications, the front surface should be designed to minimize reflection and maximize absorption by efficient coupling of light into obliquely propagating modes.

Many different approaches have been formulated to model grating structures. All of these approaches start from the Floquet expansion of the scattered and transmitted fields in terms of the grating wavevector,

$$k_n = k_0\left(\sin(\theta) + n\frac{\lambda}{d}\right);\ k_0 = \frac{2\pi}{\lambda} \quad (1)$$

where θ is the angle of incidence, d the grating period, and λ the wavelength. For calculations, the expansion must be truncated at a finite n determined by period and incident wavelength. A commonly used approach is rigorous coupled wave analysis (RCWA) [11] in which the inhomogeneous dielectric constant $\varepsilon(x)$ in the grating region is expanded into a Fourier series that couples the reflection and transmission modes. A commercially available code (G-Solver) [18] based on RCWA was used to model the gratings used in the devices reported here. Figure 4 shows a G-Solver simulation of reflection and transmission as a function of wavelength from a planar Si surface. At normal incidence both TE and TM results are identical. For example in Fig. 4 at λ=700nm the surface reflection is ~33%, leaving ~67% of the irradiance energy to be transmitted and absorbed into the substrate where it creates electrons-hole pairs.

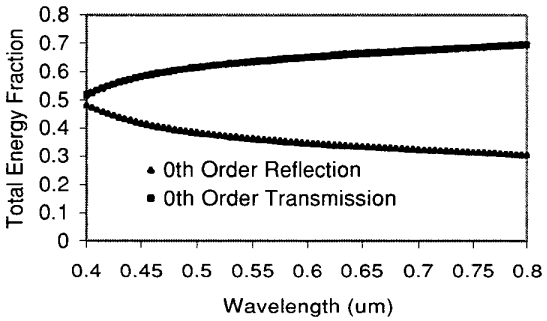

Fig. 4: Simulation of 0th diffraction order reflection and transmission for a planar (polished) Si surface as a function of wavelength.

For a periodic nanostructured Si surface with triangular shaped structures Fig. 5 shows a G-solver simulation of several transmitted diffraction orders as a function of wavelength for the TE polarization. Only the positive diffraction orders are shown in Fig. 5. At normal incidence the positive and negative orders are identical by symmetry. Similar plots can be simulated for the TM polarization.

Figure 6 plots the sum of all reflected and transmitted diffraction orders, and the absorption in the nanostructured grating region. Note the surface reflection (Fig.6) for these triangular structures is only ~4%. In the next section we will apply these simulations in an attempt to explain the photoresponse enhancement of the structured MSM PDs with respect to the planar MSM PDs.

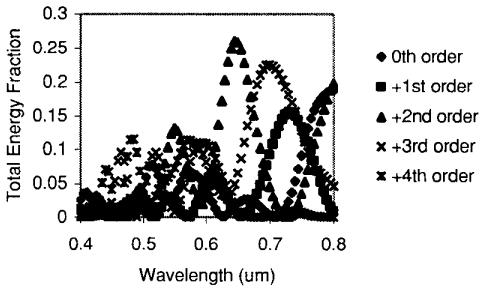

Fig. 5: Simulation of the transmission positive diffractive orders as a function of wavelength for TE polarization.

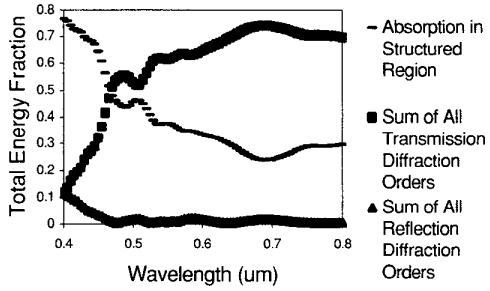

Fig. 6: Simulation of the sum of all transmission diffraction orders, sum of all reflection orders and absorption in the nanostructured grating region as a function of wavelength.

4. DC Response

The DC spectral characterization was performed using a cw xenon lamp source, ¼ meter monochrometer, polarizer, chopper, and a lock-in amplifier. The photoresponse signal for the structured MSM PDs was normalized to the photoresponse signal of the planar MSM PDs. Since the structured and planar devices were identical in all aspects except for the grating structures in the active region, we expect the normalized signal to accurately describe the effects of grating nanostructures on the device performance.

The normalized photoresponse for the triangular shaped structures as a function of wavelength is shown in Fig. 7 for both TE and TM polarizations. Figure 7 demonstrates a broadband improvement of ~2X over the entire visible spectrum for the structured device relative to the planar device. This improvement cannot be entirely attributed to the reduced (~4%) reflection of the grating surface. Since the total light transmitted is ~67% and ~96% respectively for planar and nanostructured surfaces, the estimated photo-enhancement should be ~1.4X.

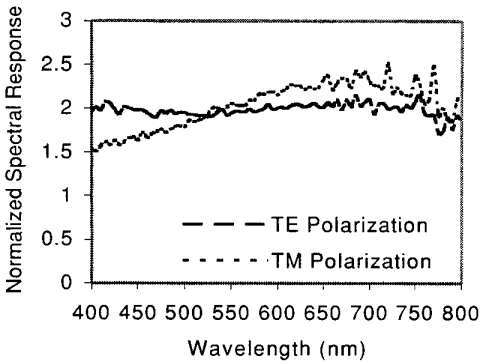

Fig. 7: Experimental spectral normalized photoresponse of triangular shaped nanostructured MSM PD with respect to similar planar devices for TE and TM polarizations.

The rigorous coupled wave analysis (RCWA) model simulations in the section 3 provide insight on reflection, transmission and absorption changes caused by the structures in the semiconductor which help explain this ~2X photoresponse enhancement. Also a significant amount of absorption occurs in the nanostructured region due to the resonant structures that concentrate the optical field close to the surface as can be seen from Fig. 6. From the diffraction grating equation, the propagation angle of the transmitted diffraction orders are calculated using

$$\theta_t=\sin^{-1}(m\lambda/dn) \qquad (2)$$

where θ_t is the angle of propagation, m is the diffractive order, λ is the optical wavelength, n is the index of the material and d is the period of the grating structures. Since the carrier collection efficiency in MSM PDs is higher for carriers generated closer to the surface due to the stronger electric fields and shorter path lengths, therefore the carriers originating from the absorption in the grating region and higher order diffraction modes propagating closer to the surface efficiently contribute to the total device photocurrent in contrast to the 0^{th} order component that creates electron-hole pairs deep inside the bulk region. Experimentally the planar MSM PD photocurrent measured at λ=700nm was ~57μA for a normally incident irradiance power density of ~1.067W/cm^2. This measurement corresponds to an internal quantum efficiency of ~63%. A photocurrent of ~60μA is theoretically calculated for the planar MSM PD using standard photocurrent models [19,20] available in literature. This results is in good agreement with our measurement.

At the same wavelength (λ=700nm) the triangular shaped structured MSM PD measured photocurrent was ~103μA for the same incident irradiance power density which corresponds to an internal quantum efficiency of ~80%. Using photocurrent models, the triangular shaped structured MSM PD decomposes the incident irradiance into grating absorption and transmission diffractive order components (fig. 5 & 6): ~4% reflection, ~25% absorption in the nanostructured region, 0^{th} order contains ~1% of the incident irradiance propagating normally into the substrate, 1^{st} order contains ~17% of the incident irradiance propagating at ~15°, 2^{nd} order contains ~9% propagating at ~30°, 3^{rd} order contains ~43% of the incident irradiance propagating at ~45°, and 4^{th} order contains ~1% of the incident irradiance propagating at ~75°. If we individually calculate the photocurrent for each diffractive order, and the absorption in the structured region and add up the values we obtain a theoretical value of photocurrent ~94μA. This result is also in good agreement with the experimental data.

In summary, the nanostructuring of Si surface significantly impacts the optical absorption of the semiconductor material resulting in enhanced photoresponse.

5. Time Response

Another beneficial aspect of the carriers being generated closer to the surface is the faster carrier collection time due to the shorter distances and higher electric fields closer to the surface. The time response characteristics of the structured devices with respect to the planar devices will help determine this qualitatively.

The time response measurements were taken using 150 fs duration pulses at λ=900nm from a mode-locked Ti:Al_2O_3 laser (0.24mW average power, 77MHz repetition rate). Detectors were probe tested using an 18GHz probe and a sampling oscilloscope. Physical constraints of the mount and probe restricted the laser spot size to no smaller than ~20μm diameter. Although the spot size was much larger than the interdigitated electrode gap, the results still show improvement for the structured devices. Pulse responses for both detectors at 2.5V bias are shown in Fig.8. The decay time in the planar device response results from carriers solely created by the 0^{th} order absorption that extends normally into the bulk region. Once these photogenerated carriers are created they diffuse into the high field depletion region of the device near the surface and are then collected. The typical minority carrier lifetime (~0.1-1ms) is several orders of magnitude larger than the diffusion time, as it can be seen from the Fig.8. The amplitude of the structured device response is almost two times larger than that of the planar device, suggesting contributions from carriers generated in the structured region due to the resonant structures and the carriers being generated by

the higher diffraction order modes that propagate closer to the surface.

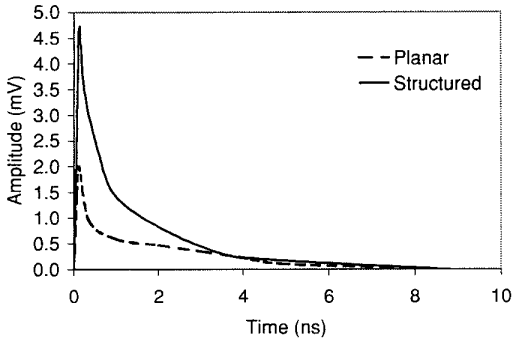

Fig. 8: Time response signals of planar and structured (triangular shape) MSM PDs for TE polarization at λ=900nm.

The contribution from the nanoscale structures enhances significantly the overall signal amplitude, and by itself it exhibits a much shorter decay time constant due to the fact that the carriers are generated in the high field region near the surface of the active region. The experimentally calculated time decay constant of the planar device is ~1.7ns and the nanostructured device is ~0.6ns at λ=900nm. Nevertheless, the overall decay time of the structured device response is almost identical to that of the planar device since it is primarily dictated by the 0^{th} diffraction order that propagates normally into the substrate region and results in slow carrier diffusion toward the surface. This measurement suggests that the fabrication of the nanostructured MSM detectors on SOI material would result in a much faster time response with amplitude comparable or larger to that of bulk devices. The results shown in Fig.8 are consistent with the DC measurements which indicate that the majority of the absorption occurs closer to the surface region for detectors with structured active areas as modeled using RCWA.

6. Summary and Conclusion

We investigated the optical reflection, transmission and absorption properties of Si nanoscale structures aimed at improving the performance of bulk silicon MSM PDs. MSM PDs were fabricated with and without nanostructures in the active area for comparison purposes. Interferometric lithography was used for the nanoscale structures and conventional optical lithography was used for patterning the device active areas as well as the metal contact regions. Devices characterized had 150X150μm^2 area with 10μm interdigitated electrode gaps.

A commercial (G-Solver) code based on rigorous coupled wave analysis was used to model the reflection and transmission diffraction orders as a function of wavelength. The energy and angle of transmission of the transmitted diffraction higher order modes as a function of nanostructure geometry is the key mechanism that improved the device performance by generating carriers near the surface of the active region. The internal quantum efficiency increased from ~67% to ~80% at λ=700nm for devices integrated with triangular shaped nanostructures. This is novel approach that shows that the effective quantum efficiency of a silicon photodetector can be increased by structuring the surface region of the semiconductor material using physical optics scales smaller than a wavelength. By increasing the absorption near the surface we not only increase the total carrier collection efficiency but also improve the time response of the signal. This improvement is shown by the time response data signals at λ=900nm which shows the fast decay of the signal originating from the grating absorption and higher diffraction orders photo-generated carriers. However the diffusion tail component of the time response signal, originating from the 0^{th} order mode, is comparable in both planar and structured devices at the same absorption depth. In order to improve the overall time response signal we need to investigate a structured design that completely isolates the carriers from being collected from these deep absorption sites. For future work we propose to fabricate the nanostructures on silicon on insulator (SOI). The two main points that we hope to accomplish in the future work are the truncation of the longer time response signal component and to optimize the design of the structures theoretically as well as experimentally to concentrate the optical field even at the critical wavelength.

Acknowledgments

The authors would like to thank A. Frauenglass for assisting in the setting up of the spectral measurement setup; Y. Wo for assisting in the automation of the monocrometer using LabView.

References

[1] P. N. J. Dennis, Photodetectors: An introduction to Current Technology, Plenum Press, 1985.
[2] M. Ghioni, F. Zappa, V. P. Kesan, and J. Warnock, "A VLSI-compatible high-speed silicon photodetector for optical data link applications,"IEEE Trans. Elect. Dev., ED-**43**, pp. 1054-1060, 1996.
[3] J. S. Wang, C. G. Shih, W. H. Chang, J. R. Middleton. P. A. Apostolakis, and M. Feng, "11 GHz bandwidth optical integrated revcievers using GaAs MESFET and MSM technology," IEEE Photon. Tech, Lett. **5**, pp. 316-318, 1993.

[4] A. Sayles and J. Uyemura, "An optoelectronic CMOS memory circuit for parallel detection and storage of optical data," IEEE J. Solid State Circuits, Sc-**23**, pp. 1110-1115, 1991.
[5] B. W. Mullins, S. F. Soares, K. A. McArdle, C. Wilson, and S. R. J. Brueck, "A simple high-speed Si Schottky diode," IEEE Photon. Tech. Lett. **3**, pp. 360-362, 1991.
[6] S. Alexandrou, C. Wang, T. Hsiang, M. Y. Liu, and S. Y. Chou, "A 75 GHz silicon metal-semiconductor-metal Schottky photodiode," Appl. Phys. Lett. **62**, pp. 2507-2509, 1994.
[7] Y. L. Ho and k. S. Wong, "Bandwidth enhancement in Si metal-semiconductor-metal photodetectors by trench formation," IEEE Photon. Tech. Lett. **8**, pp. 1064-1066 (1996).
[8] Li-Hong Laih, Tien-Chang Chang, Yen-Ann Chen, Wen-Chin Tsay, and Jsy-Wong Hong, "Characteristics of MSM photodiodes with trench electrodes on p-type Si wafer," IEEE Trans. Elect. Dev., ED-**45**, pp. 2018-2023, 1998.
[9] M. Y. Liu, E. Chen, and S. Y. Chou, "140 GHz metal-semiconductor-metal photodetectors on silicon-on-insulator substrate with a scaled layer," Appl. Phys. Lett. **65**, pp. 887-888, 1994.
[10] H. C. Lee and Bart Van Zeghbroeck, "A novel high-speed silicon MSM photodetector operating at 830 nm wavelength," IEEE Trans. Elect. Dev., ED-**16**, pp. 175-177, 1995.
[11] M. G. Moharam and T. K. Gaylord, J. Opt. Soc. Amer. **71**, 818 (1981).
[12] Saleem H. Zaidi, S.R.J. Brueck, F.M. Schellenberg, R.S. Mackay, K. Uekert, and J.J. Persoff, "Interferometric lithography exposure tool for 180-nm structures," SPIE 3048, pp.248-254, 1997.
[13] L. F. Johnson, G. W. Kammlott, and K. A. Ingersoll, "Generation of periodic surface corrugations," Appl. Opt. **17**, pp. 1165-1181, 1978.
[14] Saleem H. Zaidi and S. R. J. Brueck, Multiple exposure interferometric lithography," J. Vac. Sci. Technol. **B 11**, 658, 1993.
[15] Saleem H. Zaidi, S.R.J. Brueck, T. Hill and R.N. Shagam, "Mix and match interferometric and optical lithographies for nanoscale structuring," SPIE-3331, 406, 1988.
[16] S. Wolf and S.N. Tauber, "Silicon Processing," vol-1.,Lattice Press.
[17] S. Kemme, S.H. Zaidi, and J.M. Gee, 9th workshop on c-Si Mat., and Proc., Breckenridge (1999).
[18] Grating Solver Development Company, P.O.Box 353, Allen, TX 75013.
[19] Laurence W. Cahill, "Modeling of MSM Photodetectors", SPIE, Vol.3629, pp.453-460, Jan. 1999.
[20] L.W.Cahill, "Techniques for the design and simulation of interdigitated MSM photodetectors," Proceedings of SPIE, Vol. 2999, pp.79-85, Feb.1997.